Effect of Alloying Elements on the Solidification Characteristics and Microstructure of Al-Si-Cu-Mg-Fe 380 Alloy

S. GOWRI and F.H. SAMUEL

The effect of varying the major alloying elements within the limits of specification on the solidification behavior, fluidity, and microstructure of a 380 alloy has been studied at two cooling rates. The thermal analysis technique has been used to study the solidification behavior. The alloying elements investigated ranged from 3.22 to 4.09 pct copper, 1.01 to 1.70 pct iron, 0.06 to 0.50 pct magnesium, 1.69 to 3.00 pct zinc, and 0.16 to 0.46 pct manganese. The results show that the solidification behavior of the 380 alloys is complicated, and the cooling curve at 0.4 °C/s indicates six reactions taking place during the process of solidification. Cooling curves obtained for each of the alloying element additions, their analysis, and the resultant microstructures are discussed.

I. INTRODUCTION

THE Al-Si-Cu ternary alloy system represents the greatest volume of aluminum alloys used by the die-casting industry. The most popular alloy in this system is the 380 alloy.[1,2,3] This combines the best of both Al-Cu and Al-Si binary alloys as copper alone does not render die-casting ability to aluminum, but in conjunction with silicon, enhances the strength of the die-castable Al-Si alloys. Other alloying elements present relatively in considerable amounts are zinc, iron, magnesium, and manganese. Chromium may also be present. Each of these elements confers a particular property: copper improves room and elevated temperature properties;[1,4] magnesium makes the alloy strong, hard, and responsive to heat treatment;[5–12] iron gives strength and also prevents adhesion to steel dies (die soldering);[1–3,13] while manganese (depending on the amount) iron content, and cooling rate can prove to be beneficial or harmful. The impurities and the alloying elements partly go into solid solution in the matrix and partly form intermetallic compounds during the solidification of the metal.

The properties of the 380 alloys are determined by the fineness of the microstructure and the distribution of the phases. Two major factors which affect these are the alloy solidification rate and the alloy composition. Alloy solidification rate controls the fineness of the structure and is governed by the casting process used, *i.e.*, sand, permanent mold, die casting, *etc.* The form and distribution of the phases is controlled by the concentration of the main alloying elements and impurities present. Composition variation within the specification can have a significant effect on the microstructure and, hence, the properties. Also, the solidification sequence is influenced to a considerable extent by the interaction of the alloying elements like iron, silicon, manganese, copper, zinc, and magnesium.

S. GOWRI, Research Associate, and F.H. SAMUEL, Research Professor, are with the Department of Applied Sciences, University of Quebec at Chicoutimi, Chicoutimi, PQ, Canada.

Manuscript received April 21, 1993.

The presence of a high amount of alloying elements in 380 alloys complicates the solidification process, and there is a need to understand the role of each element and how it affects the properties and the interrelationship between these elements to achieve optimum properties.

The purpose of this study is to evaluate the effect of varying the major alloying elements within the specification limit and solidification rate on the solidification behavior, microstructure, and distribution of phases in 380 alloys. The alloying elements investigated are copper, zinc, magnesium, manganese, and iron, and the cooling rates are 0.4 and 10 °C/s. Studies of this nature are not available in literature. The only published work of this type to the authors' knowledge is that of Backerud *et al.*[14] They studied the solidification behavior of about twelve 380-type alloys, collected from various sources, to elucidate the influence of certain alloying elements on the microstructural development as a part of their research on solidification characteristics of aluminum foundry alloys. The solidification behavior and structure have been discussed by them for each of the alloys separately. Their results, however, do not compare or conclude the effect of varying the alloying elements, starting with the same base alloy.

In the present study, the solidification process has been studied by thermal analysis and supplemented by subsequent metallographic examination of the solid sample. In order to understand the state of existence of various alloying elements, experiments were planned to follow the process at two cooling rates, 0.3 and 25 °C/s, comparable to sand casting and near die-casting conditions. In our previous studies on A356 and 319, with the existing setup, we could achieve a cooling rate in the range of 20 to 30 °C/s.[15,16] With the same conditions in 380 alloys, however, a cooling rate of only 10 °C/s could be achieved, instead of the expected near die-casting cooling rate. This rate is closer to the permanent mold casting. Reasons for not attaining similar rates are discussed. Results obtained at both cooling rates are presented.

Table I. Chemical Composition of the As-Received 380 Alloy

Alloy	Elements (Wt Pct)								
	Cu	Fe	Mg	Mn	Si	Ti	Zn	Ni	Cr
Standard	3.00 to 4.00	1.00 to 1.30	0.10	0.50	7.50 to 9.50	—	3.00	—	—
Actual	3.22	1.01	0.06	0.16	9.18	0.02	2.28	0.04	0.03

II. EXPERIMENTAL PROCEDURE

The base 380 alloy was supplied by Alcan Ingot Alloys Canada, Guelph, Ontario, Canada, with the chemical composition shown in Table I. The alloys were supplied in the unmodified form.

About 6.0 kg of base material was remelted, and to each melt, measured quantities of various alloying elements such as copper, zinc, magnesium, iron, and manganese were added in the form of master alloys to obtain the final composition shown in Table II. The compositions were chosen in such a way that they fall within the composition limit indicated in the specification. In the present study, levels chosen were 3.22 (base), 3.43, and 4.09 pct copper; 0.06 (base), 0.23, and 0.50 pct magnesium; 2.28 (base), 1.69, and 3.00 pct zinc; 1.00 (base), 1.30, 1.50, and 1.70 pct iron; and 0.16 (base) and 0.46 pct manganese. The silicon level was not varied as the alloy supplied had a high silicon level, and in 380 alloys, the higher the silicon, the better the properties.

The melt was degassed at 740 °C for 20 minutes by passing dry argon through a lance. The hydrogen level of the melt after degassing was found to be about 0.14 mL/100 g of aluminum, using an AlSCAN hydrogen analyzer.

No melt treatment such as modification or grain refinement was used as these treatments are not generally required in die-casting operations, where the high cooling rate itself causes the necessary structural refinements.

The degassed metal was poured into two different molds, a graphite mold of 2.0-in. diameter maintained at 400 °C and a long cylindrical water-circulated metallic mold of 1.0-in. diameter maintained at about 14 °C. This arrangement permitted obtaining two different cooling conditions. The cooling curves were recorded by placing a thermocouple (K type) at the center of the mold and the data acquired using a Labtech/Notebook acquisition system capable of acquiring data at a rate of 900 readings/s. For samples cooled in the graphite mold, an acquisition rate of 5 readings/s and for samples cooled in the metallic mold, an acquisition rate of 20 readings/s were used in the present study.

Table II. Chemical Composition of the As-Cast Materials

Alloys	Elements (Wt Pct)				
	Cu	Fe	Mg	Mn	Zn
Base	3.22	1.01	0.06	0.16	2.28
Manganese	—	—	—	0.46	—
Iron	—	1.30	—	—	—
	—	1.50	—	—	—
	—	1.70	—	—	—
Magnesium	—	—	0.23	—	—
	—	—	0.50	—	—
Copper	3.43	—	—	—	—
	4.09	—	—	—	—
Zinc	—	—	—	—	1.69
	—	—	—	—	3.00

The analysis of the cooling curves are supplemented by metallography and phase analysis. The specimens were polished near the thermocouple region and etched for microstructural observations (optical and scanning electron microscopy [SEM]). The different phases present in the samples were identified by an electron probe microanalyzer (EPMA), operating at a voltage of 15 kV.

III. RESULTS

A. *Base Alloy*

The thermal analysis curves recorded for the base alloy at the two cooling rates are shown in Figures 1(a) and (b), with the corresponding derivative curve superimposed on the main curve. The derivative curves are generally used to determine accurately the temperature and duration of phase formation during the solidification process.

The average solidification rate dT/dt was calculated from the cooling curves according to the values of T and t at 600 °C and 450 °C by the following relationship:

$$\frac{dT}{dt} = \frac{(T_{600} - T_{450})}{(t_{600} - t_{450})}$$

where T and t represent the temperature and time, respectively. The average cooling rate obtained in the case of the heated graphite mold was taken to be 0.4 °C/s and that in the metallic mold as 10 °C/s. The actual cooling rates varied somewhat in each case (0.36 to 0.6 in graphite and 9.9 to 12.2 °C/s in metallic mold) either due to the variation of latent heat with composition or a slight variation in the experimental conditions.

At the lower cooling rate, the cooling curve shows six reactions occurring during the alloy solidification process. The liquidus temperature of the base alloy is found to be 575.1 °C (reaction 1). At this point, the primary crystals of α aluminum begin to grow. The cooling curve also shows peaks at 567.8 °C (reaction 2), eutectic reaction at 564.4 °C (reaction 3), and posteutectic reactions of a very weak peak at 523 °C (reaction 4), 492.8 °C (reaction 5), and 464.6 °C (reaction 6). From the published results,[14] these peaks are identified to correspond to the following sequence of reactions:

Reaction 1 Development of dendritic network (α aluminum).

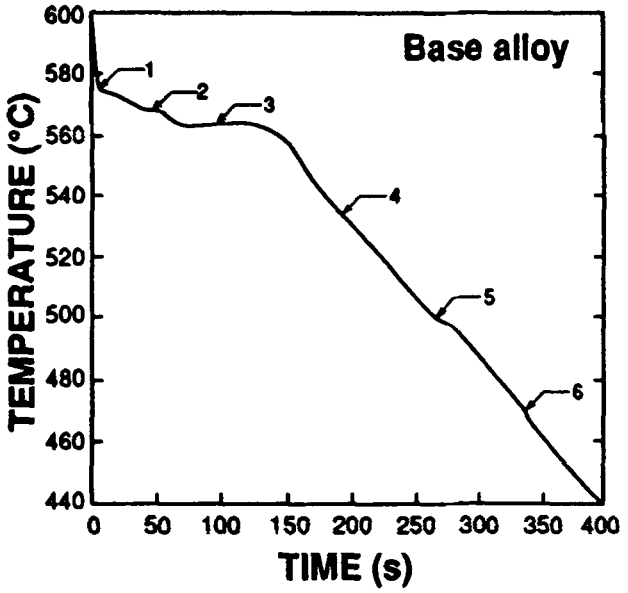

(*a*)

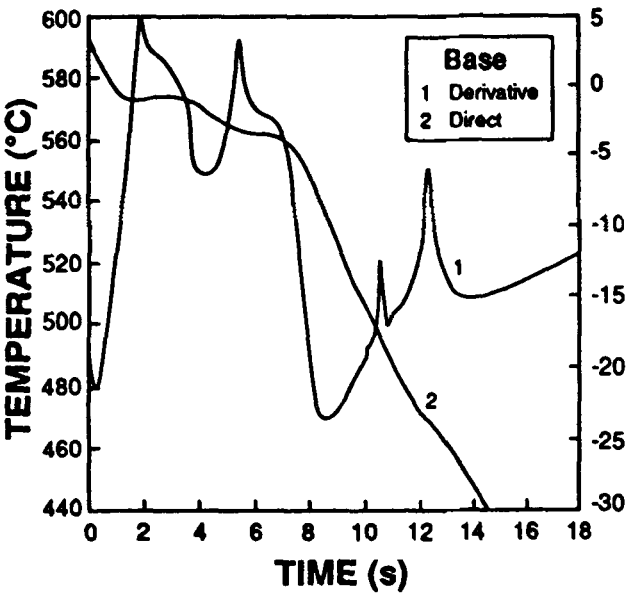

(*b*)

Fig. 1—Cooling curves obtained for the base alloy: (*a*) 0.4 °C/s, various reactions indicated; and (*b*) 10.0 °C/s, derivative curve superimposed.

2 Precipitation of iron-containing phases, Al_5FeSi and Al_{15} (Fe, Mn)$_3Si_2$.
3 Main eutectic reaction involving silicon- and iron-containing phases.
4 Precipitation of Mg_2Si.
5 Precipitation of Al_2Cu.
6 Formation of eutectics containing Al_2Cu and $Al_5Mg_8Si_2Cu_2$.

The last reaction is evident only at slower cooling rates. As the rate increases, it is seen that the reaction temperatures are shifted to lower temperatures and that not all reactions appear on the curve.

Typical microstructure of 380 alloys at a cooling rate of 0.4 °C/s is shown in Figure 2. Apart from the silicon eutectic structure, the phases observed in the base alloy are the two forms of iron phase, large amounts of copper complex, and primary silicon. The two forms of iron precipitates are the needlelike β phase represented by the formula Al_5FeSi and the Chinese scriptlike α phase represented by the formula $Al_{15}(Fe, Mn)_3Si_2$. Their form of presence depends to a great extent on the cooling rate and amount of iron and manganese present in the alloy.

At the higher cooling rate (Figure 3), it is seen that the precipitates are refined. Figures 2 and 3 together illustrate the difference in primary aluminum cell size resulting from the two cooling rates.

B. *Iron*

One impurity which is almost always present in aluminum is iron. It is picked up easily by molten aluminum from the furnace pots, ladles, and inserts. The solubility of iron and other alloying elements in aluminum is very low. As a result of this, during solidification, liquid in the interdendritic regions gets enriched with alloying materials, and iron forms complex intermetallic compounds with aluminum, silicon, manganese, and chromium. These are insoluble complexes and their volume percentage increases with an increase in iron content.

When the iron complex exists as long needles (β phase), it makes the alloy brittle and weak in mechanical properties.[1] Its presence in the Chinese script (α phase) form, however, is relatively less harmful. Therefore, in both sand and permanent mold-casting processes, where the presence of needles are observed under the casting conditions, iron level is specified to a value below 0.5 pct.

The size and shape of the iron phases can be controlled by decreasing the amount of iron, by increasing the cooling rate, or by adding an appropriate amount of neutralizers like manganese, chromium, and cobalt.[1]

For a number of reasons, in die-casting alloys, a higher percentage of iron is tolerated. At the high cooling rates prevailing in the die-casting process, iron compounds are refined and exist as fine needles. In fact, an iron content up to 1.3 pct has been found to be beneficial in terms of improved strength, hardness, and tendency toward hot cracking.[3] Another important reason for allowing a higher level of iron is that it reduces the tendency of the metal to weld or solder to the die surface, which can cause tearing of the casting surface. However, the level cannot be increased freely to harness these benefits.

Figures 4(a) and (b) show the cooling curves obtained for the iron-containing alloys. It is seen from the curves that iron changes the solidification behavior, particularly in the pre-eutectic region. As the iron content is increased, a double hump is seen. The iron phases begin to form just below the liquidus temperature, and this may be acting together with the primary phase solidification to cause this hump. The curves also indicate that the liquidus and eutectic temperatures are increased as the amount of iron is increased.

Figure 5 shows that as the iron content increases, both

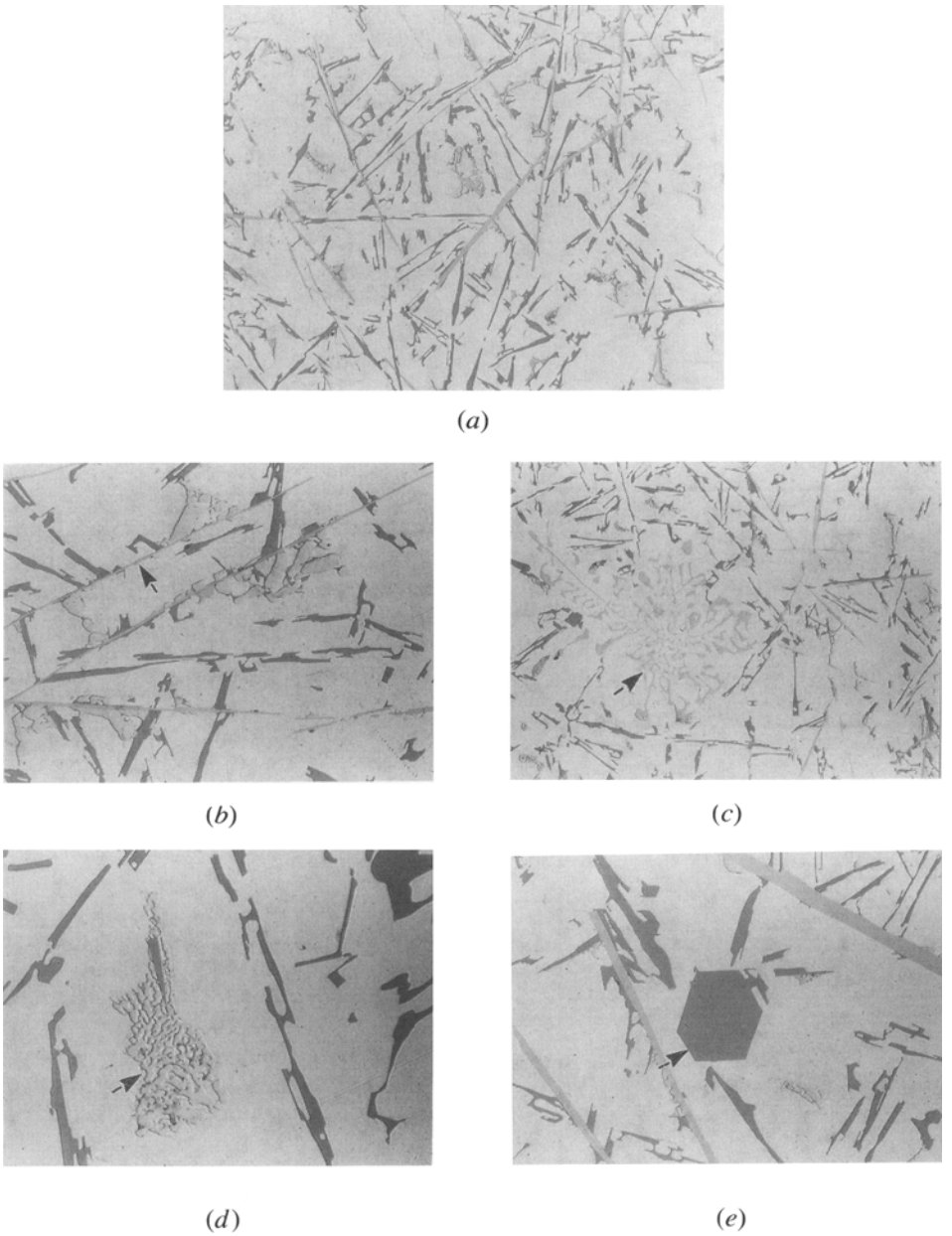

Fig. 2—Microstructures of 380 alloys and the typical appearance of the major constituents at a cooling rate of 0.4 °C/s: (*a*) general microstructure with eutectic silicon (magnification times 200); (*b*) β-iron phase needles (magnification times 500); (*c*) α-iron phase Chinese script (magnification times 200); (*d*) copper complex (magnification times 1000); and (*e*) primary silicon (magnification times 500).

the amount and size (length) of the needles increase. At higher iron levels, in a few cases, very thick and short needles shown in Figure 6 are observed, which was identified to be an AlFeMnCrSi type phase.[17]

C. *Manganese*

A small amount of manganese is always present in aluminum alloys. In Al-Si alloys, many times manganese is often specifically added to control the morphology of iron precipitates that form during solidification. When the iron content exceeds 0.45 pct in sand and permanent mold castings, as a rule of thumb, the iron:manganese ratio is maintained at 2:1.

Manganese is always considered in relation to iron in die-casting alloys, where, at the low-holding/casting temperature, the element also combines with iron and chromium to form a *sludge*. Sludge is harmful as it is hard and abrasive. In 380 alloys, since chromium is present in a small concentration, and iron is required to be maintained around 1.0 to 1.3 pct, only the manganese level can be adjusted to have an allowable sludge factor (SF) of 1.8, where the SF is defined by[18]

$$SF = x \text{ pct Fe} + 2\,x \text{ pct Mn} + 3\,x \text{ pct Cr}$$

This formula, commonly referred to as the 123 rule (iron:manganese:chromium), is only a guide and can vary with different producers and users.

The formation of the sludge is also a function of the holding temperature. Sludge, when formed in the liquid

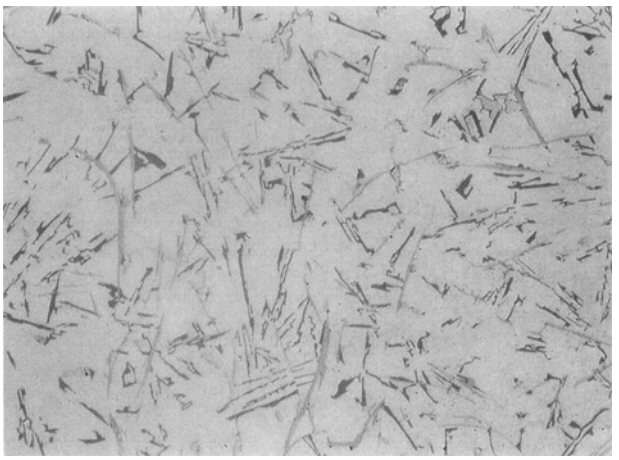

Fig. 3—Microstructure of the base alloy: cooling rate ≈10 °C/s, (magnification times 500).

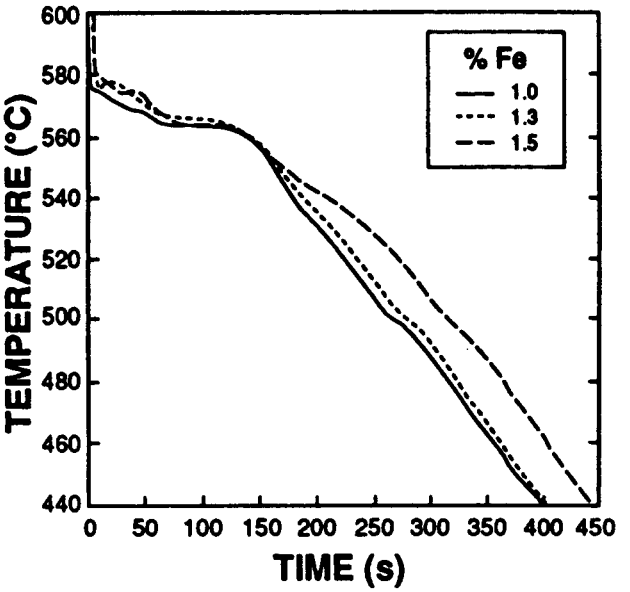

(*a*)

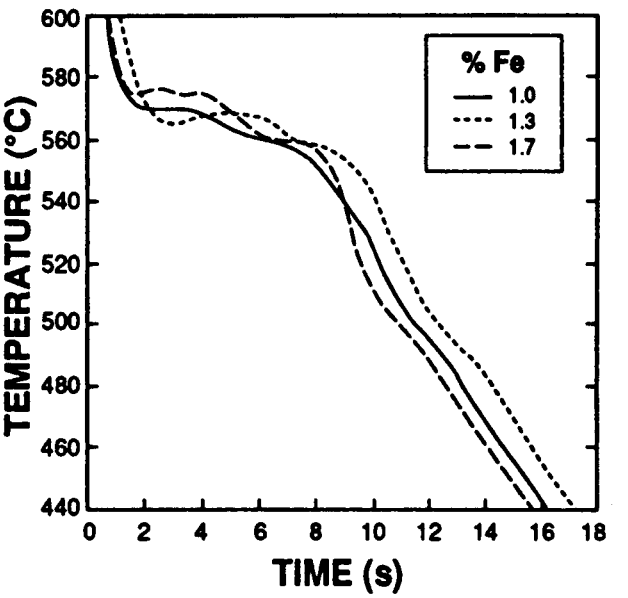

(*b*)

Fig. 4—Cooling curves obtained for the iron-containing alloys: (*a*) 0.4 °C/s and (*b*) 10 °C/s.

state, tends to sediment to the bottom of the crucible as its density is higher than that of the liquid aluminum, particularly when held for a long time. Gobrecht[18] made experiments with 380 alloys where he varied iron, manganese, and chromium and related the SF factor to the holding temperature. He showed that a critical temperature exists below which the sedimentation (formation of sludge and settling to the bottom) occurs. Figure 7 shows his results. By maintaining the holding temperature above the critical temperature or an agitated bath, a sludge factor higher than 1.8 can be tolerated.

The α-iron phase which forms during solidification and the sludge which forms during the holding period have the same chemical formula, $Al_{15}(Mn, Fe)_3Si_2$, but vary in morphology. The condition under which this phase forms before the dendrites to cause sludging is a function of iron, manganese, and silicon content. Figure 8 shows a simplified phase diagram indicating the compositions under which the $Al_{15}(Mn, Fe)_3Si$ is expected to form primarily. Backerud *et al.*[14] have shown the effect of manganese, iron, and silicon additions on the solidification sequence in 380 alloys in their atlas.

The percentage manganese in the as-received material was low at 0.16 pct (iron:manganese 6:1) such that the SF was 1.42. In most 380 alloy specifications with iron in the range of 1.0 to 1.3 pct manganese is specified at about 0.5 pct (iron:manganese 2.6:1). In order to compare the microstructure and solidification progress at the standard ratio 2:1, manganese was added to the base alloy so as to achieve a final composition of 0.5 pct and the solidification curve recorded. The chemical analysis of the alloy indicated a manganese content of 0.46 pct.

Figures 9(a) and (b) show the cooling curves obtained for the two different iron:manganese levels at the two cooling rates studied. At the high cooling rate, it is very clear that the increase in manganese increases both the melting point and the eutectic temperature by 4 °C.

A noticeable difference is observed between the base and the high manganese-containing alloys toward the end of solidification. This suggests that manganese, besides affecting the shape and form of the iron precipitates, also has an influence on the copper complexes.

Microstructural observations of the two alloys (Figure 10) show the effect of increasing manganese. The high-manganese alloy shows an additional star-shaped phase which was identified by EPMA analysis as sludge. Inspite of the high holding and casting temperature used in the present study, sludge is still seen to form in these alloys.

D. *Magnesium*

In the 380 alloys, much of the research has been focussed on the effect of magnesium on the properties. The

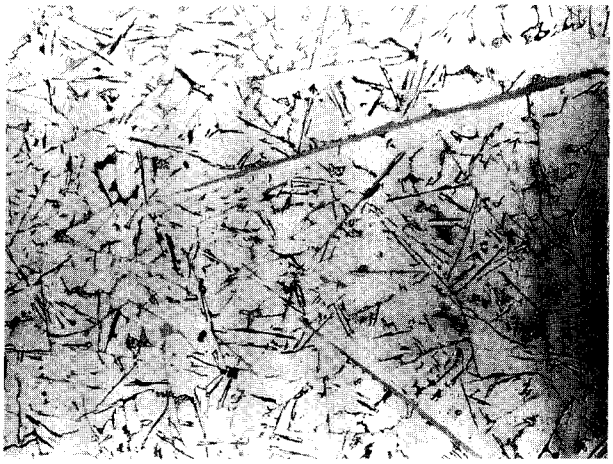

(*a*)

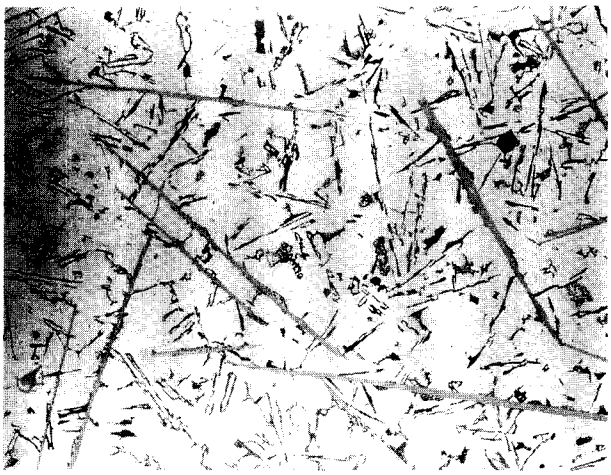

(*b*)

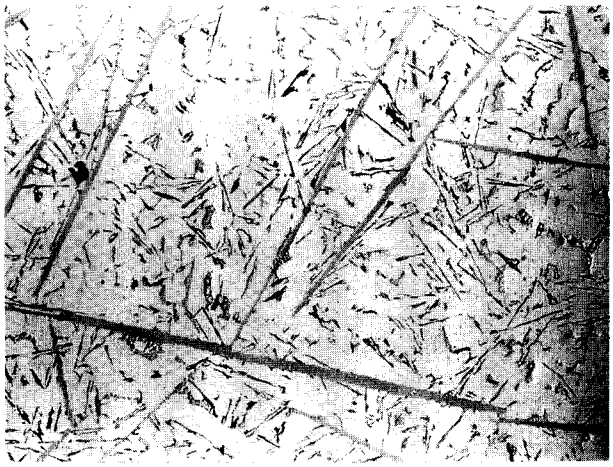

(*c*)

Fig. 5—Microstructures of the iron-containing alloys obtained at a cooling rate of 0.4 °C/s: (*a*) 1.3 pct iron; (*b*) 1.5 pct iron; and (*c*) 1.7 pct iron (magnification times 100).

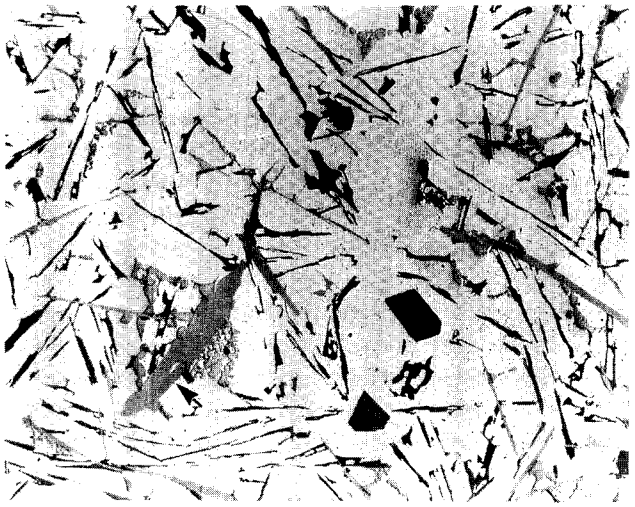

Fig. 6—Microstructure of the high iron-containing alloy showing the AlFeMnCrSi-type precipitate (magnification times 200).

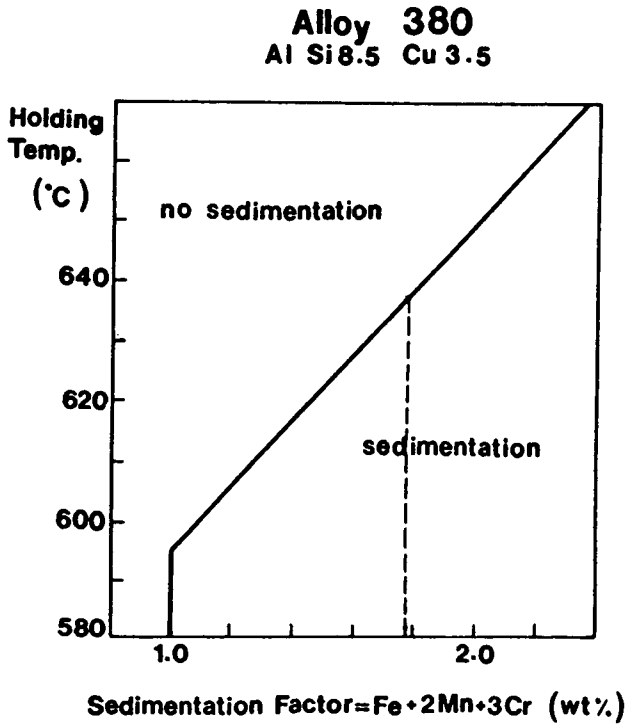

Fig. 7—Simplified phase diagram for 380-type alloys showing the region where $Al_{15}(Fe, Mn)_3Si_2$ is expected to form primarily.[14]

allowable amount of magnesium in the North American specification is 0.1 pct max, whereas European specifications allow 0.3 pct max. Since the majority of the die-casting alloys are produced from secondary sources (scrap) which inherently contain a higher percentage of magnesium, it becomes a heavy burden on the part of secondary smelters to remove excess magnesium. Even though magnesium can be removed easily by passing chlorine or halogens, the process is not environmentally friendly and requires additional overhead costs to contain the pollutants. Therefore, there has been an active campaign to change the allowable level of magnesium

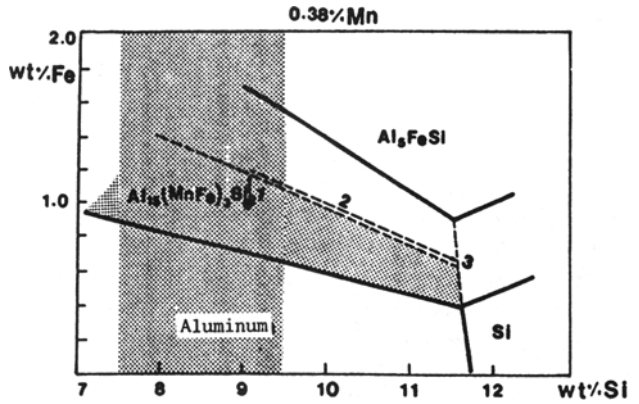

Fig. 8—Temperature *vs* sedimentation factor, according to Gobrecht.[18]

in North American alloys. Inspite of the numerous studies done to establish the beneficial effect of increasing magnesium on the mechanical and machining properties,[5-12,19] the specification still stands at 0.1 pct max here.

Our initial studies were focussed on the effect of magnesium in the range of 0.10 to 0.50 pct on the solidification behavior of two 380 alloys supplied by different alloy producers. The results[20] showed that the increase in magnesium up to 0.30 pct did not affect the solidification behavior. The eutectic temperature changed approximately 1 °C for each 0.10 pct of added magnesium. The results of the present study reiterate the same observations. The cooling curves obtained for 0.06, 0.23, and 0.50 pct magnesium are shown in Figures 11(a) and (b). The curves fail to show the peak corresponding to the Mg_2Si phase. The copper phase (reaction 4) temperature is seen to be shifted to a lower temperature.

As the magnesium level is increased, the amount of α phase present in the microstructure is seen to increase, and the needles appear thick and short. Inspite of the high-magnesium content, the Mg_2Si phase was not visible in the microstructure shown in Figure 12.

E. *Copper*

The addition of copper to binary Al-Si alloys improves the strength of the castings.[1,3] Copper in these alloys is present as Al_2Cu or as a complex precipitate with aluminum, magnesium, and silicon. The final complex that is present in the microstructure depends on the percentage of these elements in addition to that of copper.

The copper range in the specification is 3.00 to 4.00 pct. We varied copper from 3.22 pct (base) composition to 3.43 and 4.09 pct. The resulting cooling curves for the three compositions are shown in Figures 13(a) and (b) at the two cooling rates.

It is observed that increasing copper decreases the melting point considerably. The eutectic temperature is also reduced. The phase formation temperature of Al_2Cu, however, is increased.

The effect of increasing copper on the microstructure of 380 alloys is shown in Figure 14. It is observed that as the copper content is increased, the agglomerations shown in Figure 2 are seen to be broken, and the size

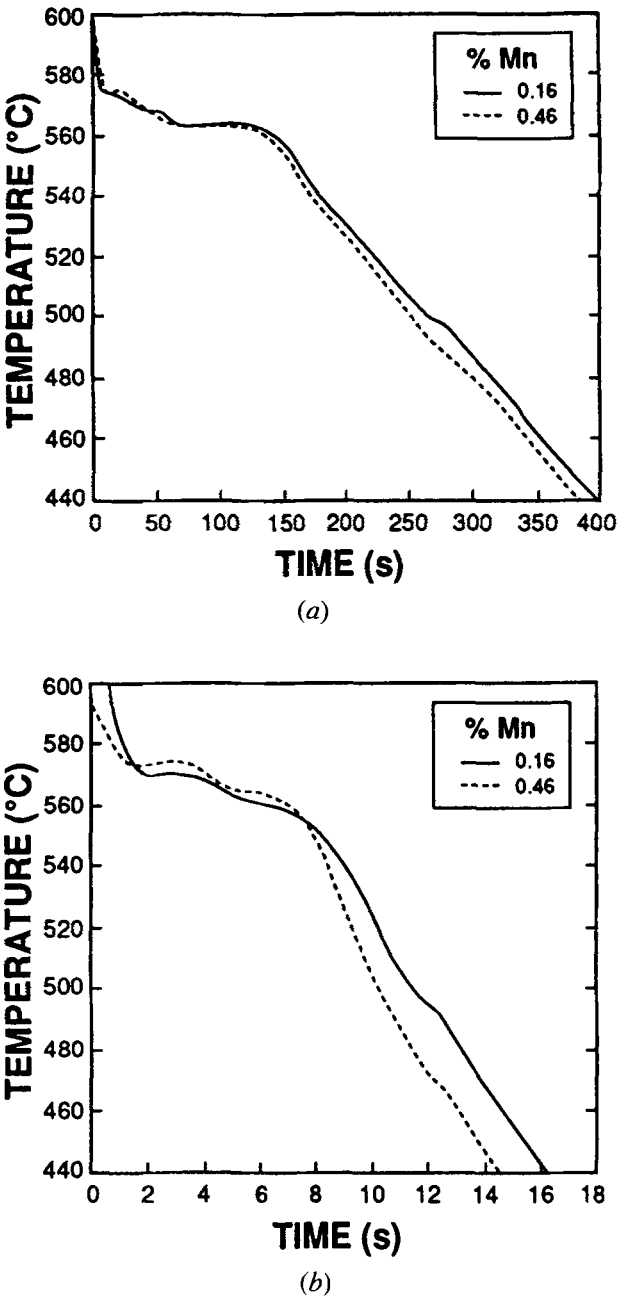

Fig. 9—Cooling curves obtained for the manganese-containing alloys: (*a*) 0.4 °C/s and (*b*) 10 °C/s.

of the precipitates decreases. Primary silicon crystals were seen dispersed in the microstructure. At 4.09 pct copper, in addition to these precipitates, a blocky copper phase (marked in Figure 14(c)) is observed.

F. *Zinc*

Zinc has a relatively high solubility in aluminum both at high temperature and at room temperature. Zinc up to 3.00 pct has been reported to have no pronounced effect on the properties of Al-Si alloys.[1,3,13] The role of zinc is not well understood, and it is believed that it may improve the high-temperature properties,[4] besides machinability.[21]

During solidification, zinc successively goes into solid

(*a*)

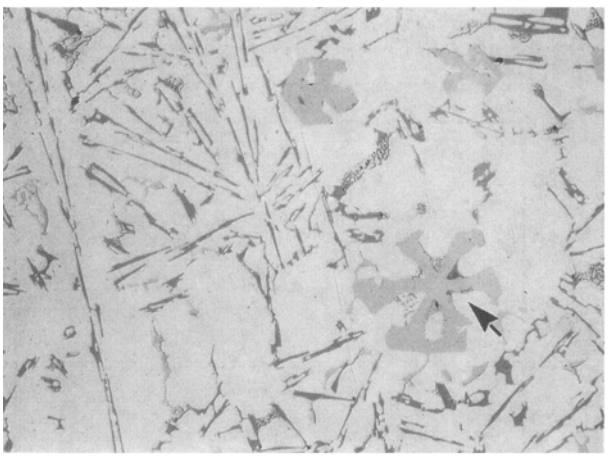

(*b*)

Fig. 10—Microstructures of manganese-containing alloy obtained at a cooling rate of 0.4 °C/s: (*a*) 0.16 pct manganese and (*b*) 0.46 pct manganese, (magnification times 200).

solution, and it is therefore expected to alter only the liquidus region. The cooling curves (not presented) show that zinc lowers the melting point. The eutectic temperature at both cooling rates is not very much affected by the different levels of zinc.

IV. DISCUSSION

The results obtained in our study show the solidification behavior of 380 alloys at conditions close to sand and permanent mold castings. Similar information, at least closer to die-casting conditions, certainly would have been beneficial. Failure to achieve high cooling rates similar to those obtained in 319 or 356 alloys in our earlier studies is believed to be associated with the high heat of solidification of 380 alloys.

The latent heat (LH) released during the solidification of pure aluminum is 94.5 cal/g,[1] and this heat increases with an increase in the silicon content.[17] The LH of solidification, for example in A356 (6.00 pct silicon), 380 (9.00 pct silicon), and 390 (17.00 pct silicon) is 242, 376, and 430 cal/g, respectively.[17,22] As a result of its higher silicon content, solidification of 380 alloys requires removal of more heat than 356 (or 319) alloys. Therefore, for the same casting conditions, this alloy will solidify at a much slower rate than 319 or A356. In other words, in order to achieve the same cooling rate during solidification in all three alloys, extra cooling arrangements must be made for the 380 alloys than for the other two alloys.

The liquidus temperature of the 380-base alloy in this study is found to be 575.1 °C. The reported value of the liquidus of the AA standard alloy in a previous study is 573 °C.[14] Liquidus temperature and other thermal analysis parameters are sensitive to composition variation. Since the values are dependent on chemical composition, and since there is a wide variation in percentage of alloying elements possible that are allowed in the specification, even among 380 alloys, no attempts are made to compare the present results of thermal analysis with those published in the literature.

The results show that the addition of alloying elements changes the eutectic and posteutectic temperatures, and the magnitude of change is a function of the alloy content. The effect of changes in the chemical composition on these temperatures is shown in Table III. The differences, even though they appear small, when translated in terms of solidification range and fraction of solid can have a significant effect on the final properties of the alloy. For example, copper reduces the eutectic temperature significantly, and therefore, the freezing range is increased. The level of porosity in the alloy has been related to the length of the freezing range.[23]

To monitor the effect of varying the alloying elements on the melt characteristics, fluidity measurements were made. The fluidity, measured by the distance that the alloy flows through the tube (in a Ragone Fluidity Tester) prior to solidification, is shown in Table IV as a function of the additive elements. The fluidity values did not vary drastically so as to allow for a definite relationship. Table IV shows that an increase in copper increases the fluidity, while an increase in iron decreases it. As the iron content increases, it is postulated that higher amounts of iron-bearing needles affect the feeding characteristics adversely.[24] The insensitivity to show significant differences in fluidity could be due to the higher silicon content of the alloy which already imparted higher fluidity to the melt. Therefore, we propose that fluidity is not a sensitive test to correlate the variation in alloying elements in 380 alloys.

Table V compares the influence of the various elements Zn, Mg, Cu, Mn, and Fe in the refinement of microstructures, as indicated by the size of dendrite-arm spacing (DAS), for the same cooling conditions. An increased level of the alloying content decreases the DAS.

The EPMA analysis of the matrix in the various alloys indicated the presence of about 1.30 to 2.00 pct silicon, 0.50 to 1.30 pct copper, and 2.20 pct zinc. The cooling curves, particularly at the lower cooling rate, clearly indicate the presence of most of the reaction products, except for the iron-bearing compounds (considering the amount of iron in the alloy). Iron forms insoluble phases with three of the main elements, namely, aluminum, silicon, and manganese, and the temperature of formation

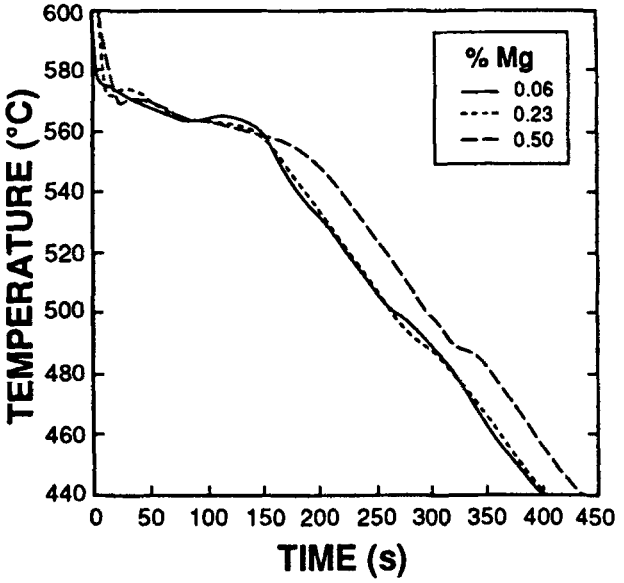

(*a*)

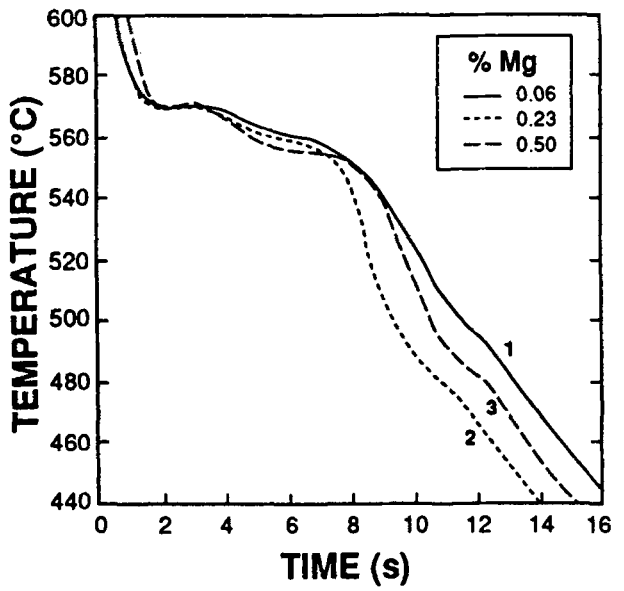

(*b*)

Fig. 11—Cooling curves obtained for the magnesium-containing alloys: (*a*) 0.4 °C/s and (*b*) 10 °C/s.

of these compounds, which is a function of both the iron:manganese ratio and cooling rate, lies in the range of 571 °C to 561 °C. This temperature, which lies between the liquidus and eutectic reaction, due to the small amount of heat liberated during that reaction, often merges with the primary solidification reaction and is difficult to detect from the cooling curves.

With the increase in iron concentration, the amount of β phase increases and the constituents become larger and more numerous. At all increased iron levels, the iron precipitates were found to be only of β type. The EPMA analysis of the needle phase (base alloy) yielded a composition of 73.00 pct aluminum, 13.40 pct iron, 13.50 pct silicon, and 0.89 pct manganese at the low cooling rate and 64.82 pct aluminum, 16.35 pct iron, 17.80 pct silicon, and 1.67 pct manganese at 10 °C/s. As the cooling rate increases, the proportion of different elements forming the needle phase is seen to increase, changing the stoichiometry of the phase. Even though the needle phase is reported to dissolve a limited amount of copper,[14] we did not detect copper in our results.

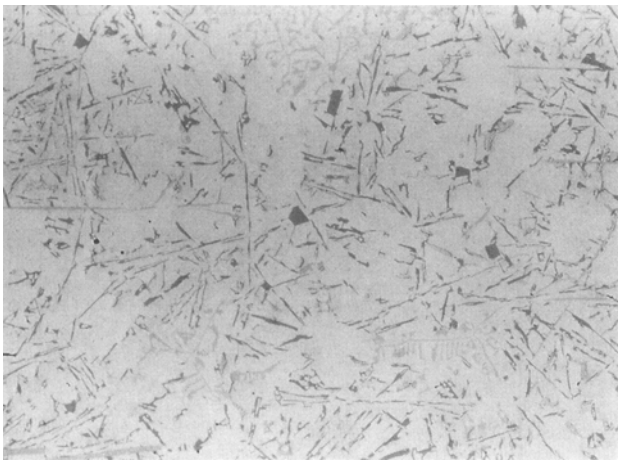

Fig. 12—Microstructure of 0.23 pct magnesium-containing alloys obtained at a cooling rate of 10 °C/s; (magnification times 500).

As discussed in Section III, manganese is added to convert the iron needles to the less harmful Chinese script form. Our observation of the microstructure indicates that inspite of maintaining the ratio at 2:1, the amount of α phase in the microstructure was not markedly increased and that the β phase was still the major constituent. Instead, manganese was seen to be precipitated with iron and chromium as sludge. The composition of the sludge was analyzed to be 60.00 pct aluminum, 21.90 pct iron, 8.20 pct silicon, 7.40 pct manganese, and 0.60 pct chromium with 1.90 pct copper.

The SF of the base alloy used in the present study was 1.42. Our results also shows that inspite of iron being one of the principal constituents of the sludge, for an increase in iron level up to 1.70 pct (with a SF of 2.11), the microstructure did not reveal sludge but merely an increased amount of β phase. Inspite of the high holding temperature (100 °C above the critical temperature reported by Gobrecht[18]) and short holding time (30 minutes after the melting), sludge phase was seen to form. Thus, one important element that needs to be controlled critically in die-casting alloys is manganese.

Also, increasing manganese does not necessarily result in the α phase. As evident from the microstructure of a high-manganese alloy (Figure 10), iron constituents still appear as needles. This is probably because manganese is primarily consumed in the formation of sludge and not enough is left to form the α phase during solidification.

While manganese is added to control the microstructure, copper and magnesium are added to make the alloy heat-treatable. In order to do so, a minimum of 3.00 pct copper is required. Three kinds of precipitates can form when magnesium and copper are present, namely, Al_2Cu, Mg_2Si, and $Al_5Mg_8Cu_2Si_2$.

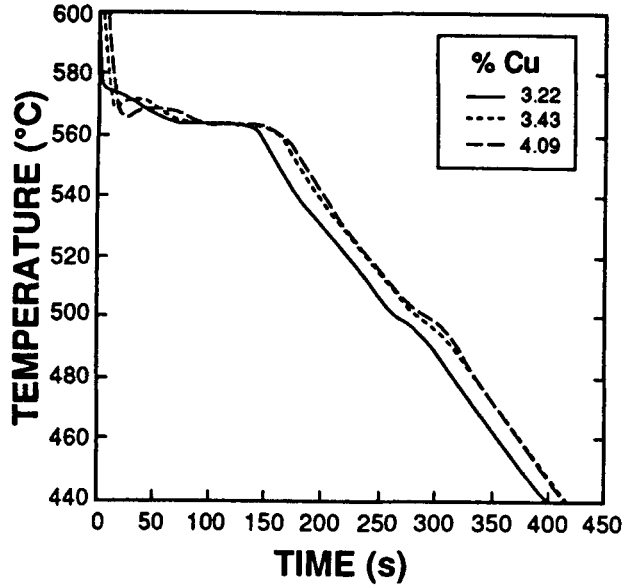

(*a*)

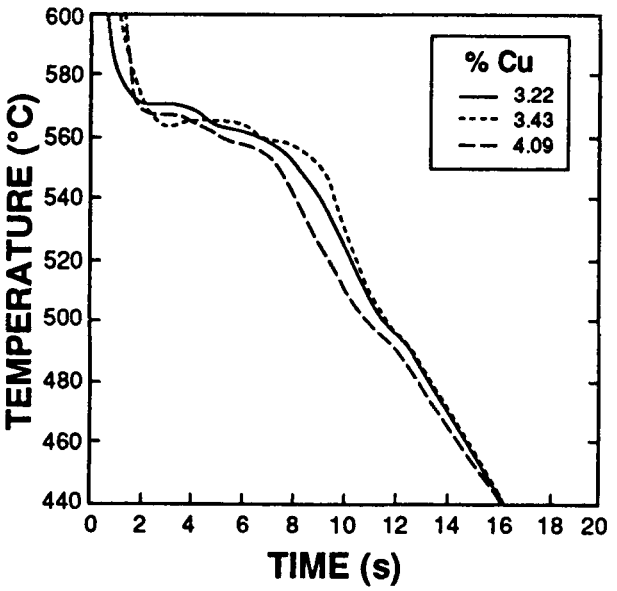

(*b*)

Fig. 13—Cooling curves obtained for copper-containing alloys: (*a*) 0.4 °C/s and (*b*) 10 °C/s.

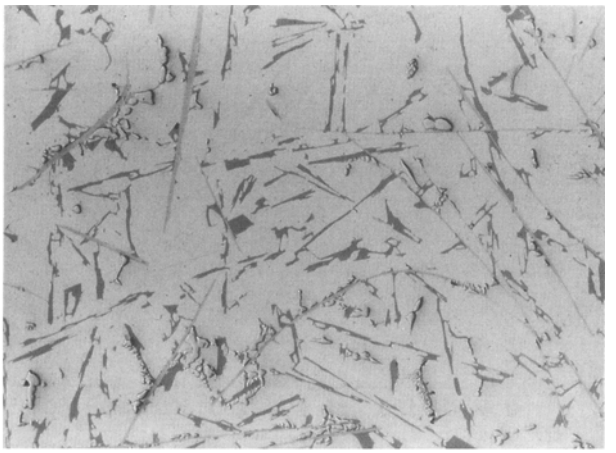

(*a*)

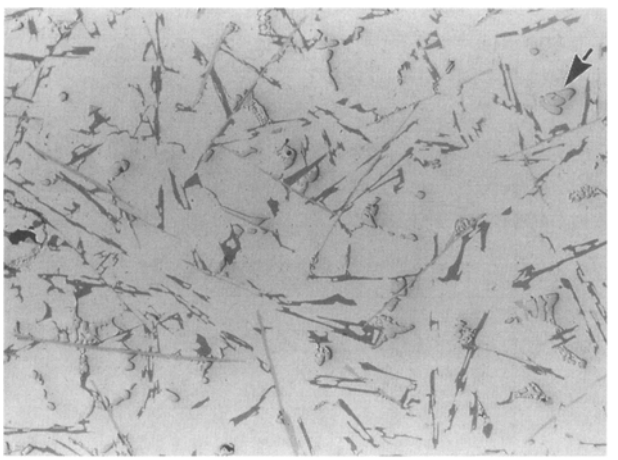

(*b*)

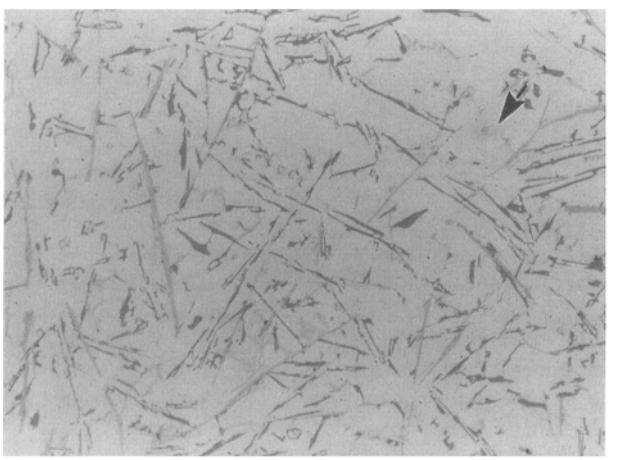

(*c*)

Fig. 14—Microstructures of copper-containing alloys: (*a*) 3.3 pct copper at a cooling rate of 0.4 °C/s (magnification times 200); (*b*) 4.09 pct copper at a cooling rate of 0.4 °C/s (magnification times 200); and (*c*) 4.09 pct copper at a cooling rate of 10 °C/s (magnification times 500).

The Mg_2Si phase forms just above the copper phase formation point and is at most times not resolved in the cooling curves. It is also consumed during the last reaction (reaction 6 listed earlier). Because the solubility of Mg_2Si phase varies with temperature just as copper in aluminum, it confers a heat-treating effect on the 380 alloys.

One interesting microstructural feature observed in the case of high magnesium-containing alloys is the change in the appearance and size of the iron phases. Further studies are warranted on the effect of magnesium and iron phase formation and its dissolution behavior.

Increasing copper results in increased fluidity. The precipitate Al_2Cu occurs as clusters in the interdendritic

Table III. Effect of Alloying Elements on the Eutectic and Posteutectic Reactions

Alloy Type	Eutectic (°C)	Posteutectic Reactions (°C)
Cooling Rate = 0.4 °C/s		
Base	564.4	523.0, 492.0, 464.6
0.46 Mn	564.3	487.0
3.43 Cu	564.0	532.0, 500.5
4.09 Cu	562.8	503.0
1.69 Zn	564.7	504.4, 500.10, 477.70
3.00 Zn	563.2	498.0
1.30 Fe	566.7	501.8
1.50 Fe	564.0	501.8
1.70 Fe	564.3	491.7
0.23 Mg	563.6	492.6
0.50 Mg	561.7	488.0
Cooling Rate = 10 °C/s		
Base	560.0	496.8
0.46 Mn	564.3	469.2
3.43 Cu	559.5	496.2
4.09 Cu	556.0	499.5
1.69 Zn	566.8	525.0, 497.0
3.00 Zn	559.0	495.3
1.30 Fe	558.8	493.2
1.50 Fe	556.0	514.9, 505.8
1.70 Fe	560.0	497.0
0.23 Mg	560.3	487.0
0.50 Mg	556.5	484.0

Table IV. Effect of Alloying Elements on the Fluidity of the 380 Alloys

Alloy Type	Fluidity (cm)	
	740 °C	680 °C
Base	43.0	31.5
0.46 Mn	42.0	31.0
3.43 Cu	43.4	—
4.09 Cu	45.3	—
1.69 Zn	43.2	30.4
3.00 Zn	41.1	—
1.30 Fe	43.8	—
1.50 Fe	42.1	32.3
1.70 Fe	39.6	32.0
0.23 Mg	43.8	—
0.50 Mg	43.2	32.7

Table V. Effect of Alloying Elements on the DAS of the 380 Alloy

Alloy Composition	DAS (μm)	
	0.4 °C/s	10.0 °C/s
Base	66.9	19.5
0.46 Mn	56.3	18.7
3.43 Cu	60.6	14.64
4.0 Cu	48.7	17.75
1.6 Zn	56.43	—
3.0 Zn	48.3	16.3
1.3 Fe	48.4	13.6
1.5 Fe	61.2	—
1.7 Fe	50.6	17.1
0.20 Mg	55.9	13.7
0.50 Mg	40.0	15.9

network. The compositional analysis of the copper complexes was difficult as they occurred as an agglomerate of phases or were too fine. The EPMA analysis indicated the presence of copper:aluminum 33.16:57.10 and magnesium:silicon 3.77:1.77 with 0.70 iron and 3.32 pct zinc.

Zinc is one of the elements that is present in die-casting alloys whose role is not well defined. It can have serious effects on the foundry characteristics, as it has a tendency to oxidize easily. Our results indicate that the solidification behavior is not affected by increasing zinc, as zinc only goes into solid solution. The EPMA analysis of the matrix of different alloys confirmed the presence of zinc in the matrix. It is, therefore, difficult to assess the effect of zinc from cooling curves alone. Fluidity is decreased as zinc is increased. The precipitation temperature of the copper complexes is shifted, and this is believed to be because zinc has some solubility in these complexes (about 4 pct). The microstructural observations revealed that the copper complexes were more spheroidized when zinc was increased.

V. CONCLUSIONS

The results of our study show that the initial chemical composition of the alloys exerts a strong influence on the solidification behavior and the different phases formed. In 380 alloys, where there are many alloying elements specifically added to conform certain properties, our results show that even slight changes in the concentration can cause a variation in the reaction temperature and resultant microstructures.

Our results reveal that increasing iron beyond that of a specified SF of 1.8 to 2.1 did not result in the formation of sludge, but merely resulted in increasing the amount of the β iron phase. However, increasing manganese to maintain a specified 2:1 (iron:manganese) ratio, resulted in the precipitation of sludge in the microstructure. Inspite of the high holding temperature and the short holding time used in the present study, sludge was seen to form. This shows that manganese plays a more important role in the formation of the sludge than iron and that it requires a more critical control in die-casting alloys.

Our results also indicate that in the high magnesium-containing alloys (0.23 pct or more), the appearance and size of the iron-containing phases is changed, pointing to the possible influence of magnesium on both the α and β phases. Further studies in this direction would be useful.

The results of the fluidity measurements show that an increase in the copper and magnesium level increases the fluidity marginally, while zinc and iron decreases it. The insensitivity to show any significant difference is attributed to the higher silicon content of the starting alloy which already imparted higher fluidity. Therefore, in our opinion, fluidity is not a sensitive test to assess the melt characteristics in 380 alloys.

ACKNOWLEDGMENTS

The authors would like to acknowledge the financial support received from the Natural Sciences and

Engineering Research Council of Canada (NSERC), the Fondation Sagamie de l'Université du Québec à Chicoutimi and the Société d'électrolyse et de chimie Alcan (SECAL).

REFERENCES

1. *Metals Handbook*, 8th ed., ASM, Metals Park, OH, 1961, vol. 1.
2. *Aluminum*, K.R. Van Horn, ed., ASM, Metals Park, OH, 1967, vol. 1.
3. R.W. Bruner: *Die Casting Alloys*, SDCE Supplement, Warren, MI, 1976.
4. E.G. Morgan: *Foundry Trade J.*, 1982, June, pp. 887-90.
5. P.R. Dunn and W.Y. Dickert: *Die Cast. Eng.*, 1975, vol. 19, pp. 12-17.
6. Warren Johnsson: *SDCE Trans.*, Paper No. 73, 1964.
7. R.C. Harris, S. Lipson, and H. Rosenthal: *AFS Trans.*, 1956, vol. 64, pp. 470-81.
8. R. DasGupta, C.C. Brown, and S. Marek: *AFS Trans.*, 1989, vol. 97, pp. 245-254.
9. J.E. Vorren, J.E. Evensen, and T.B. Pedersen: *AFS Trans.*, 1984, vol. 92, pp. 459-66.
10. R.A. Quadt and J.J. Adams: *The Foundry*, 1949, vol. 77, pp. 88-91.
11. J.L. Jorstad: *Soc. Auto. Eng., Inc.*, 1978, pp. 1-13.
12. E.K. Holz: *5th Natl Die Casting Congr.*, Detroit, MI, Paper No. 112, 1968, Nov.
13. *Wabash Alloy Data Book*, Aluminum Alloy Data Book, Publ: Wabash Alloys, Wabash, IN.
14. L. Backerud, E. Krol, and J. Tamminen: *AFS/SKAN-Aluminium*, Oslo, Norway, 1990, vol. 2.
15. S. Gowri and F.H. Samuel: *Metall. Trans. A*, 1992, vol. 23A, pp. 3369-76.
16. L. Ananthanarayanan, F.H. Samuel, and J.E. Gruzleski: *AFS Trans.*, 1992, vol. 100, pp. 383-91.
17. John L. Jorstad: *390 Alloy Technology: Foundry Characteristics*, Reynolds Metals Company, Richmond, VA, 1975, June.
18. J. Gobrecht: *Geiserei*, 1975, vol. 62 (10), pp. 263-66.
19. *Metals Handbook: Casting*, 9th ed., ASM INTERNATIONAL, Metals Park, OH, 1988, vol. 15.
20. S. Gowri and F.H. Samuel: *AFS Trans.*, Paper No. 93-145, 1993, vol. 101, in press.
21. D.L. Colwell: *AFS Trans.*, 1952, vol. 60, p. 87.
22. E.L. Pan, C.S. Lin, and C.R. Loper: *AFS Trans.*, 1990, vol. 90–117, pp. 735-46.
23. J. Zou, K. Tynelius, D.G. Kim, S. Shivkumar, and D. Apelian: *Proc. Int. Symp. on Production and Electrolysis of Light Metals*, Halifax, Aug., 1989, Pergamon Press, New York, NY, 1989, pp. 87-95.
24. H. Iwahori, H. Takamiya, K. Yonekura, Y. Yamamato, and M. Nakamura: *J. Jpn. Inst. Light Met.*, 1988, vol. 60 (9), pp. 590-95.